

Quantifying the Role of Inhibition in Associative Long-Term Potentiation in Dentate Granule Cells With Computational Models

WILLIAM R. HOLMES¹ AND WILLIAM B. LEVY²

¹Neurobiology Program, Department of Biological Sciences, Ohio University, Athens, Ohio 45701; and ²Departments of Neurological Surgery and Psychology, University of Virginia Medical School, Charlottesville, Virginia 22908

Holmes, William R. and William B. Levy. Quantifying the role of inhibition in associative long-term potentiation in dentate granule cells with computational models. *J. Neurophysiol.* 78: 103–116, 1997. In the dentate gyrus, coactivation of a mildly strong ipsilateral perforant path (pp) input with a weak contralateral pp input will not induce associative long-term potentiation in the weak input path unless both inputs project to the same part of the molecular layer. This “spatial convergence requirement” is thought to arise from either voltage attenuation between input locations or inhibition. Simulations with a detailed model of a dentate granule cell were performed to rule out voltage attenuation and to quantify the inhibition necessary to obtain the spatial convergence requirement. Strong lateral and weak medial or strong medial and weak lateral pp input were activated eight times at 400 Hz. Calcium current through *N*-methyl-D-aspartate receptor channels and subsequent changes in calcium concentration and the concentration of calmodulin bound with four calcium ions ($[\text{Cal-Ca}_4]$) in the spine head were computed for a medial and a lateral pp synapse. To satisfy the spatial convergence requirement, peak $[\text{Cal-Ca}_4]$ had to be much larger in the strongly activated path synapse than in the weakly activated path synapse. With no inhibition in the model, differences in peak $[\text{Cal-Ca}_4]$ at the two synapses were small, ruling out voltage attenuation as the explanation of the spatial convergence requirement. However, with shunting inhibition, modeled by reducing membrane resistivity to $1,600 \Omega \text{ cm}^2$ in the distal two-thirds of the dendritic tree, peak $[\text{Cal-Ca}_4]$ was 3–5 times larger in the strongly activated path synapse than in the weakly activated path synapse. The magnitude of shunting inhibition was varied to determine the level that maximized this difference in peak $[\text{Cal-Ca}_4]$. For strong lateral and weak medial pp input, the optimal level was one that prevented the cell from firing an action potential. For strong medial and weak lateral pp input, the optimal level was one at which the cell fired two action potentials. The distribution of shunting inhibition that best satisfied the spatial convergence requirement was inhibition on the distal two-thirds of the dendritic tree with or without inhibition at the soma, with inhibition stronger in the distal third than in the middle third. It was estimated that the number of inhibitory synapses involved in the shunting inhibition should be 25–50% of the number of excitatory synapses activated by the eight-pulse, 400-Hz tetanus. This number could be 20–50% of the total number of inhibitory synapses in the distal two-thirds of the dendritic tree. The addition of a single inhibitory synapse on a dendrite had a significant effect on peak spine head $[\text{Cal-Ca}_4]$ in nearby spines. Inhibitory synapses had to be activated four or more times at 100 Hz for effective shunting to take place, and the inhibition had to begin no later than 2–5 ms after the first excitatory input. The results suggest that inhibition can isolate potentiated synapses to particular dendritic domains and that the location of activated inhibitory synapses may affect potentiation of individual synapses on individual dendrites.

INTRODUCTION

Long-term potentiation (LTP) is a modification of synaptic strength first reported in the dentate gyrus (Bliss and

Lomo 1973). Its induction there is thought to depend on calcium influx through *N*-methyl-D-aspartate (NMDA) receptor channels (see Malenka and Nicoll 1993 for a review). Whether or not LTP is induced at a particular synapse depends on whether the synapse is activated concurrently with a sufficient number of other synapses to produce a voltage change that will relieve the magnesium block of the NMDA receptor channels. The voltage change at the synapse is determined by the electrotonic structure of the dendritic tree and the number and locations of coactivated excitatory and inhibitory inputs.

In the dentate there is a spatial convergence requirement for the induction of associative LTP. Inputs to the dentate from the perforant path (pp) terminate in a strict laminar arrangement: lateral pp fibers terminate in the distal third of the molecular layer, whereas medial pp fibers terminate in the middle third. Taking advantage of this arrangement, White et al. (1988, 1990) showed that mildly strong activation of the ipsilateral pp provides the postsynaptic excitation needed for associative LTP of a coactivated weak contralateral pp input when both inputs project to the same part of the molecular layer. When strong and weak inputs project to nonoverlapping dendritic domains, associative LTP of the weak input pathway does not occur.

This spatial convergence requirement can be explained if the voltage changes experienced by synapses in nonoverlapping dendritic areas are very different, but it is not clear how such a difference arises. Voltage differences might occur because of voltage attenuation along the electrotonic distance between input locations. However, simulations suggest that this does not explain the spatial convergence requirement (Yousukhno et al. 1996). Voltage differences can also occur if inhibition is activated and this inhibition shunts the dendritic depolarization and limits its spread to adjacent regions. Use of blockers of inhibition supports this explanation (Tomasulo et al. 1993; Zhang and Levy 1993), but the location and strength of this hypothesized inhibition has not been determined.

Inhibition in dentate granule cells occurs largely as the result of activation of a γ -aminobutyric acid-A (GABA_A)-receptor-mediated conductance. This type of inhibition is called shunting inhibition because the reversal potential for this conductance is close to or (depending on the preparation) positive to the resting membrane potential. Consequently, it can have little or no effect on membrane potential or in some cases it can be depolarizing. Even when the conductance is depolarizing, it is still considered inhibitory

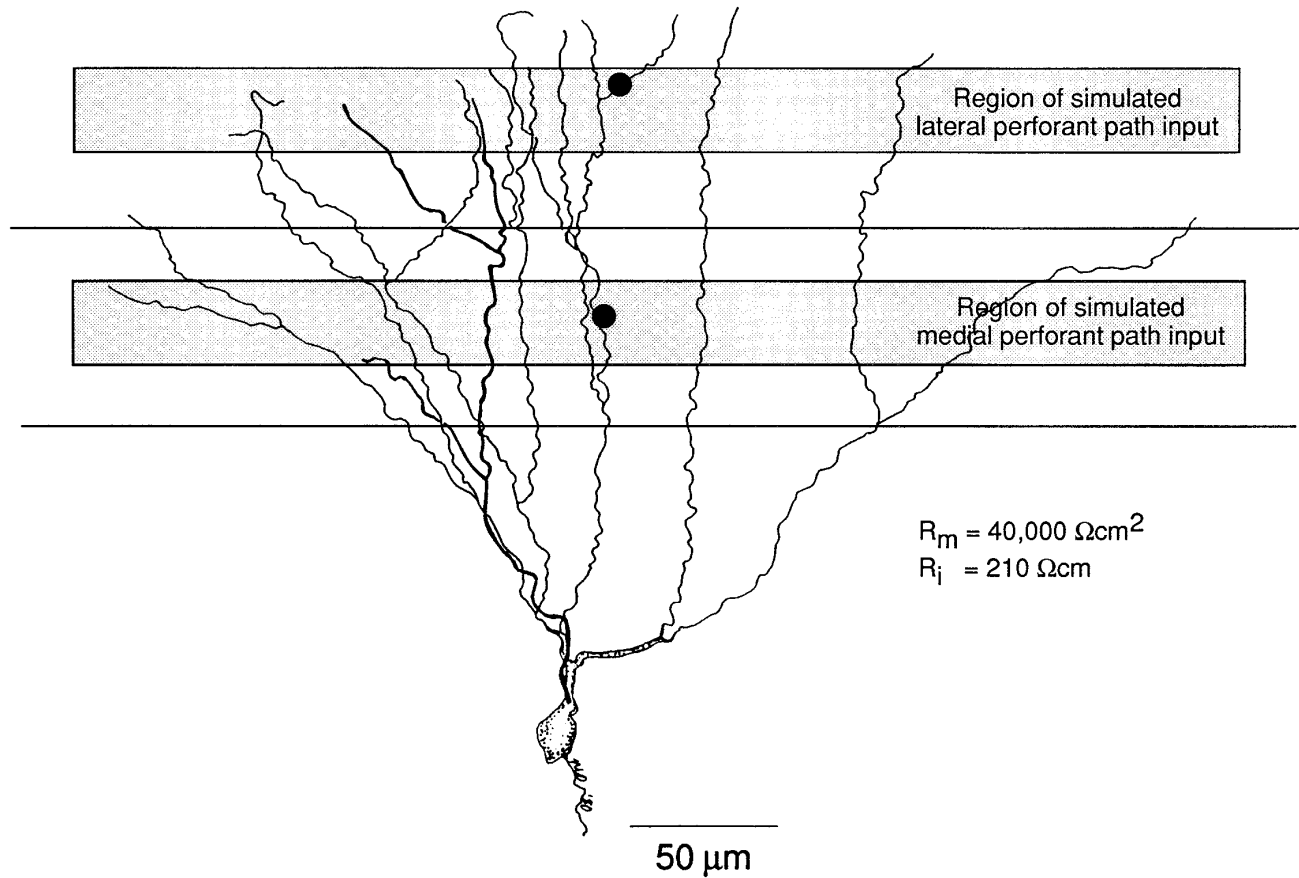


FIG. 1. Cell used in simulations. Horizontal lines: approximate boundaries separating middle third of dendritic tree from proximal and distal thirds. In simulations, medial perforant path (pp) input was activated in lower shaded region and lateral pp input in upper shaded region. ●: locations of the 2 synapses monitored in all simulations. R_m , membrane resistivity; R_i , axial resistivity.

$$AR(t) = 0.154\{[0.834 AR(0) + AR^*(0)] \exp(-0.167t) - [-5.66 AR(0) + AR^*(0)] \exp(-6.66t)\}$$

$$AR^*(t) = 0.154\{[5.66 AR^*(0) + 4.72 AR(0)] \exp(-0.167t) - [-0.834 AR^*(0) + 4.72 AR(0)] \exp(-6.66t)\} \quad (4)$$

When an inhibitory synapse is first activated, $AR(0)$ is assumed to be 60 bound receptors and $AR^*(0)$ is zero. For each subsequent activation the conductance time variable t is reset to zero and the number of receptors in the bound state is increased by $60 - AR(t) - AR^*(t)$ receptors. This ensures that the total number of receptors in the bound and open states does not exceed 60, i.e., there is receptor saturation for the GABA synapse. This kinetic scheme does not include receptor desensitization. The conductance was computed by multiplying the number of channels in the open state by 28 pS, the single-channel conductance (DeKoninck and Mody 1994). The reversal potential was assumed to be -70 mV

TABLE 1. Maximum conductance values

	Axon	Soma	Dendrite
Na	210	120	60 → 15
K	28	16	8 → 2
Ca	0	1	0.5 → 0.125
KCa	0	1	0.5 → 0.125
Leak	1.5E-3	0	0

Values are in mS/cm².

(the same as the resting potential), consistent with the value of -69 mV found by Blaxter and Carlen (1988).

SHUNTING INHIBITION. Before any inhibitory synapses were included in the model, a shunting conductance was modeled by reducing R_m in specific dendritic compartments. Initially R_m values over a large range of were tested ($100-10,000 \Omega \text{ cm}^2$) to get an idea of where the spatial convergence requirement might be satisfied. Additional R_m values over a narrower range were tested to quantify more accurately the amount of shunting inhibition needed. The R_m values that gave results most consistent with the spatial convergence requirement were used to estimate the number of inhibitory synapses activated and their frequency of activation. For a fixed frequency of activation the number of activated inhibitory synapses, N , was computed as

$$N = (1/R_{m\text{target}} - 1/R_m) * A / g_{\text{ave}} \quad (5)$$

where $R_{m\text{target}}$ is the target R_m for a particular level of shunting inhibition (e.g., $2,000 \Omega \text{ cm}^2$), R_m is $40,000 \Omega \text{ cm}^2$, A is the membrane area of the dendrite or dendritic region of interest, and g_{ave} is the average value of the synaptic conductance of a single synapse activated repetitively at a given frequency. Several sets of activation frequency and number of synapses were calculated.

Synaptic inputs and input frequency

Excitatory synapses with both NMDA and non-NMDA conductances were modeled on dendritic spines. Lateral pp stimulation was modeled as the activation of 1–336 synapses on the distal third

of the dendritic tree, whereas medial pp stimulation was modeled as the activation of 1–360 synapses in the middle third of the dendritic tree. These pathways were activated eight times at 400 Hz. The dendritic locations of activated synapses are shown in Fig. 1.

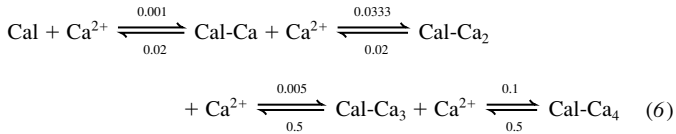
Inhibitory synapses were modeled on dendritic shafts and at the soma. These synapses were activated at 100 Hz, with the number of activated synapses being determined by Eq. 5. Although there may be direct pp inhibitory connections to dentate granule cells, it was assumed that most inhibition came from interneurons activated by pp input. Consequently, inhibitory synapses were activated after a short delay following excitatory synapse activation. The times of activation began at 2, 5, 7, and 10 ms for 100-Hz activation, with equal numbers activated at the different starting times. The group with activation beginning at 10 ms sometimes had an additional activation at 5 ms.

Spine model

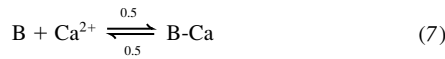
The structure of the spine model is the same as given previously (Holmes 1990; Holmes and Levy 1990a). The spine head was divided into four compartments, with the two compartments closest to the spine tip being 50 nm thick. The spine neck was divided into 4 compartments, and 12 compartments were used to represent the dendrite. The spine head was $0.55 \times 0.55 \mu\text{m}$ and the neck was $0.1 \times 0.73 \mu\text{m}$. Calcium concentration in each compartment was determined by the dynamics of calcium influx, diffusion, binding, and removal.

The calcium component of the current through NMDA receptors was computed as in the previous model (Holmes and Levy 1990a) from the total synaptic current and the relative permeabilities of Ca^{2+} , Na^+ , and K^+ ions at NMDA receptor channels (Mayer and Westbrook 1987). This method is more accurate than methods that calculate the calcium component as a straight percentage of the total NMDA-receptor-mediated current because calcium flux remains inward at potentials between the synaptic reversal potential and the calcium reversal potential. This difference may be important if action potentials invade dendritic regions with only minor attenuation.

Although calcium diffusion and removal were modeled as in the previous model, the binding reactions have been updated significantly. Calcium is assumed to bind to calmodulin and to an unspecified fast buffer. The rate constants for binding to calmodulin (in $\mu\text{M}^{-1} \text{ms}^{-1}$ and ms^{-1}) were taken from Linse et al. (1991) as follows



whereas binding to the fast buffer was simply



where the rate constants are again in units of $\mu\text{M}^{-1} \text{ms}^{-1}$ and ms^{-1} . The initial concentrations of Cal, Cal-Ca, Cal-Ca₂, Cal-Ca₃, Cal-Ca₄, and bound and free buffer were determined from the steady-state solutions of the differential equations for Eqs. 6 and 7 for given calmodulin, calcium, and buffer concentrations.

Consequently, six equations were solved over time for each compartment (*i* is the subscript for compartment *i*)

$$\begin{aligned} d[\text{Ca}]_i/dt &= -D/V_i \{ (A/\delta)_{i,i-1} ([\text{Ca}]_i - [\text{Ca}]_{i-1}) + (A/\delta)_{i,i+1} ([\text{Ca}]_i \\ &- [\text{Ca}]_{i+1}) \} + \text{influx (for compartment 1 only)} \\ &- k_{p_i} ([\text{Ca}]_i - [\text{Ca}]_i) - k_{\text{ON}i} [\text{Ca}]_i [\text{Ca}]_i \end{aligned}$$

$$\begin{aligned} &- k_{\text{ON}2} [\text{Ca}]_i [\text{Cal-Ca}]_i - k_{\text{ON}3} [\text{Ca}]_i [\text{Cal-Ca}_2]_i \\ &- k_{\text{ON}4} [\text{Ca}]_i [\text{Cal-Ca}_3]_i + k_{\text{OFF}1} [\text{Cal-Ca}]_i + k_{\text{OFF}2} [\text{Cal-Ca}_2]_i \\ &+ k_{\text{OFF}3} [\text{Cal-Ca}_3]_i + k_{\text{OFF}4} [\text{Cal-Ca}_4]_i \\ &- k b_{\text{ON}} [\text{Ca}]_i [B]_i + k b_{\text{OFF}} ([B]_i - [B]_i) \end{aligned} \quad (8)$$

$$d[\text{Cal}]_i/dt = -k_{\text{ON}1} [\text{Ca}]_i [\text{Cal}]_i + k_{\text{OFF}1} [\text{Cal-Ca}]_i$$

$$\begin{aligned} d[\text{Cal-Ca}]_i/dt &= -k_{\text{ON}2} [\text{Ca}]_i [\text{Cal-Ca}]_i - k_{\text{OFF}1} [\text{Cal-Ca}]_i \\ &+ k_{\text{ON}1} [\text{Ca}]_i [\text{Cal}]_i + k_{\text{OFF}2} [\text{Cal-Ca}_2]_i \end{aligned}$$

$$\begin{aligned} d[\text{Cal-Ca}_2]_i/dt &= -k_{\text{ON}3} [\text{Ca}]_i [\text{Cal-Ca}_2]_i - k_{\text{OFF}2} [\text{Cal-Ca}_2]_i \\ &+ k_{\text{ON}2} [\text{Ca}]_i [\text{Cal-Ca}]_i + k_{\text{OFF}3} [\text{Cal-Ca}_3]_i \end{aligned}$$

$$\begin{aligned} d[\text{Cal-Ca}_3]_i/dt &= -k_{\text{ON}4} [\text{Ca}]_i [\text{Cal-Ca}_3]_i - k_{\text{OFF}3} [\text{Cal-Ca}_3]_i \\ &+ k_{\text{ON}3} [\text{Ca}]_i [\text{Cal-Ca}_2]_i + k_{\text{OFF}4} [\text{Cal-Ca}_4]_i \end{aligned}$$

$$d[B]_i/dt = -k b_{\text{ON}} [\text{Ca}]_i [B]_i + k b_{\text{OFF}} ([B]_i - [B]_i)$$

In the first equation above, *D* is the calcium diffusion coefficient ($0.6 \mu\text{m}^2/\text{ms}$), $(A/\delta)_{i,j}$ is the coupling coefficient between compartments *i* and *j*, *V_i* is volume, *k_{p_i}* is the pump rate ($1.4 \times 10^{-4} \text{cm/s}$), and $[\text{Ca}]_i$ is 20 nM. The ON and OFF rate constants are given in Eqs. 6 and 7, total buffer concentration $[B]_i$ was 40 μM , and $[\text{Cal-Ca}_4]$ was calculated from $[\text{Cal}_{\text{total}}] - [\text{Cal}] - [\text{Cal-Ca}] - [\text{Cal-Ca}_2] - [\text{Cal-Ca}_3]$, where $[\text{Cal}_{\text{total}}]$ was 50 μM near the tip of the spine head and 25 μM elsewhere. The peak spine head calcium concentration and the peak concentration of calmodulin with four bound calcium ions ($[\text{Cal-Ca}_4]$) were used as measures of LTP induction.

RESULTS

Electrotonic distance alone cannot account for the spatial convergence requirement

The hypothesis that voltage attenuation along the electrotonic distance between input locations accounts for the spatial convergence requirement was tested. LTP stimulation paradigms modeled were pairing strong medial pp activation with weak lateral pp activation or pairing strong lateral pp activation with weak medial pp activation. A strong medial pp input was modeled as activation of 60–180 excitatory synapses in the middle third of the dendritic tree, whereas a strong lateral pp input was modeled as activation of 48–192 excitatory synapses in the distal third of the dendritic tree. Weak inputs were modeled as the activation of single synapses. There was no inhibition in this set of simulations. As in Yousukhno et al. (1996), calcium concentration was computed at activated medial and lateral pp synapses located along the same dendritic path to the soma. Here we also calculated the concentration of calmodulin fully loaded with calcium. If the voltage attenuation along the electrotonic distance between the medial and lateral pp synapses can explain the spatial convergence requirement, then peak $[\text{Cal-Ca}_4]$ should be very different in the two spine heads.

With strong medial and weak lateral pp conditioning stimulation, $[\text{Cal-Ca}_4]$ was nearly the same at the medial pp spine head and the lateral pp spine head, as shown in Fig.

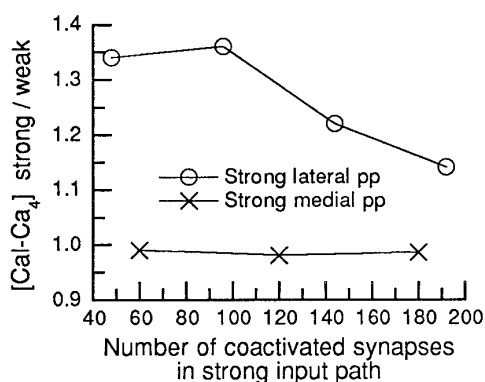


FIG. 2. Electrotonic distance between input locations does not account for spatial convergence requirement. Peak concentration of calmodulin with 4 bound calcium ions ($[\text{Cal-Ca}_4]$) in strong input path synapse divided by peak $[\text{Cal-Ca}_4]$ in weak input path synapse is shown as a function of the number of synapses activated by the strong input. Input was 8 pulses delivered at 400 Hz.

2. Potentiation in this case was judged not specific. The translaminar interaction occurred because the large voltage change generated in the middle third of the dendritic tree decayed very little with distance as it spread distally. This was expected because the electrotonic distance between the two synapses was ~ 0.2 and because of the sealed end boundary condition at the distal terminals. Because the NMDA receptor channels at the lateral pp synapse saw almost the same voltage change as the channels at the medial pp synapse, magnesium block, calcium influx, and thus peak Ca^{2+} concentration ($[\text{Ca}^{2+}]$) and $[\text{Cal-Ca}_4]$ were similar.

Likewise, laminar specificity was not obtained for the reverse interaction with strong lateral and weak medial pp input. In this case the voltages at the two synapses were different, with the voltage being more depolarized at the lateral pp synapse than at the medial pp synapse. The reason a difference was seen here and not for the reverse pairing is that voltage attenuation is greater toward the soma than away from it. Despite the larger depolarization at the lateral pp synapse, peak $[\text{Cal-Ca}_4]$ levels at medial and lateral pp synapses differed by at most 35% (Fig. 2).

Reduction in R_m (shunting inhibition) can give the spatial convergence requirement

The electrotonic distance between the medial and lateral pp synapses was small in the above simulations because R_m was $40,000 \Omega \text{ cm}^2$. If R_m in the distal two-thirds of the dendritic tree were much smaller than $40,000 \Omega \text{ cm}^2$, then the synapses might be separated far enough electrotonically from each other to give the spatial convergence requirement. A smaller R_m value could occur if the dendrites were subject to a shunting inhibition at the same time they received the excitatory input.

To test this, R_m in the distal two-thirds of the dendritic tree and the soma was set to $1,600 \Omega \text{ cm}^2$. Simulations were then performed activating either 300 medial pp synapses and 1 lateral pp synapse or 264 lateral pp synapses and 1 medial pp synapse eight times at 400 Hz.

It was found that peak $[\text{Ca}^{2+}]$ and peak $[\text{Cal-Ca}_4]$ were much higher in the strongly activated path synapse than in the weakly activated path synapse. With strong medial pp

activation peak $[\text{Ca}^{2+}]$ was 2.2 times higher and peak $[\text{Cal-Ca}_4]$ was 3.5 times higher at the strong input (medial pp) synapse than at the weak input (lateral pp) synapse (Fig. 3A). With strong lateral pp activation the corresponding ratios of peak $[\text{Ca}^{2+}]$ and peak $[\text{Cal-Ca}_4]$ at strong input synapses to weak input synapses were 2.7 and 4.8 (Fig. 3B). In both cases the difference in peak $[\text{Ca}^{2+}]$ was amplified into a larger difference in peak $[\text{Cal-Ca}_4]$. This suggested that a lower R_m , possibly caused by a shunting inhibition, could explain the spatial convergence requirement.

Optimal shunting inhibition for the spatial convergence requirement

The question was asked: what value of R_m for the soma and distal two-thirds of the dendritic tree will maximize the ratio of the peak $[\text{Cal-Ca}_4]$ values between strong and weak input path synapses illustrated in Fig. 3? To address this, the simulations above were repeated with R_m values ranging from 100 to $10,000 \Omega \text{ cm}^2$.

As shown in Fig. 4, the largest ratios were found for $R_m = 2,200 \Omega \text{ cm}^2$ when 300 medial pp synapses and 1 lateral pp synapse were activated, and for $R_m = 1,800 \Omega \text{ cm}^2$ when 264 lateral pp synapses and 1 medial pp synapse were activated. The ratios tended to rise rapidly, plateau, and then fall rapidly as R_m was increased. With very low R_m , shunting was too strong to allow much depolarization to occur, and consequently peak $[\text{Ca}^{2+}]$ and peak $[\text{Cal-Ca}_4]$ were small in both lamina. With high R_m , the depolarization was large at both the lateral pp synapse and the medial pp synapse, and this caused comparable peak calcium concentration and $[\text{Cal-Ca}_4]$ to occur.

Interestingly, the maximum ratio of peak $[\text{Cal-Ca}_4]$ values in the two laminae depended strongly on the number of action potentials generated by the strongly activated pathway. When the medial pp was strongly activated, the largest ratio occurred for the minimum R_m value that allowed two action potentials to be generated (Fig. 4A). When the lateral pp was strongly activated, the maximum ratio occurred at a point below the threshold for action potential generation (Fig. 4B). This result implies that a strong medial, weak lateral pp input should generate one or two action potentials for potentiation to occur at activated medial pp synapses but not at lateral pp synapses. However, it is not necessary for spikes to be generated by strong lateral, weak medial pp input to get potentiation at activated lateral pp synapses but not at medial pp synapses.

This dependence of the maximum ratio of peak $[\text{Cal-Ca}_4]$ values on the number of action potentials was obtained even as the number of active synapses in the strong pathway was varied (Fig. 5). When the number of synapses activated in the medial pp was reduced to 240, the largest ratio again occurred just after R_m was increased to a level that caused two action potentials to be generated. However, the ratio was reduced to 2.9, reflecting the smaller number of activated synapses (Fig. 5A). When the number of synapses activated in the lateral pp was changed to 312 or 192, again the ratio peaked at an R_m value that prevented action potential generation (Fig. 5B). The ratio rose to 5.7 with 312 synapses and was 3.6 with 192 synapses. Note that as the number of excitatory synapses was increased, the maximum ratios were

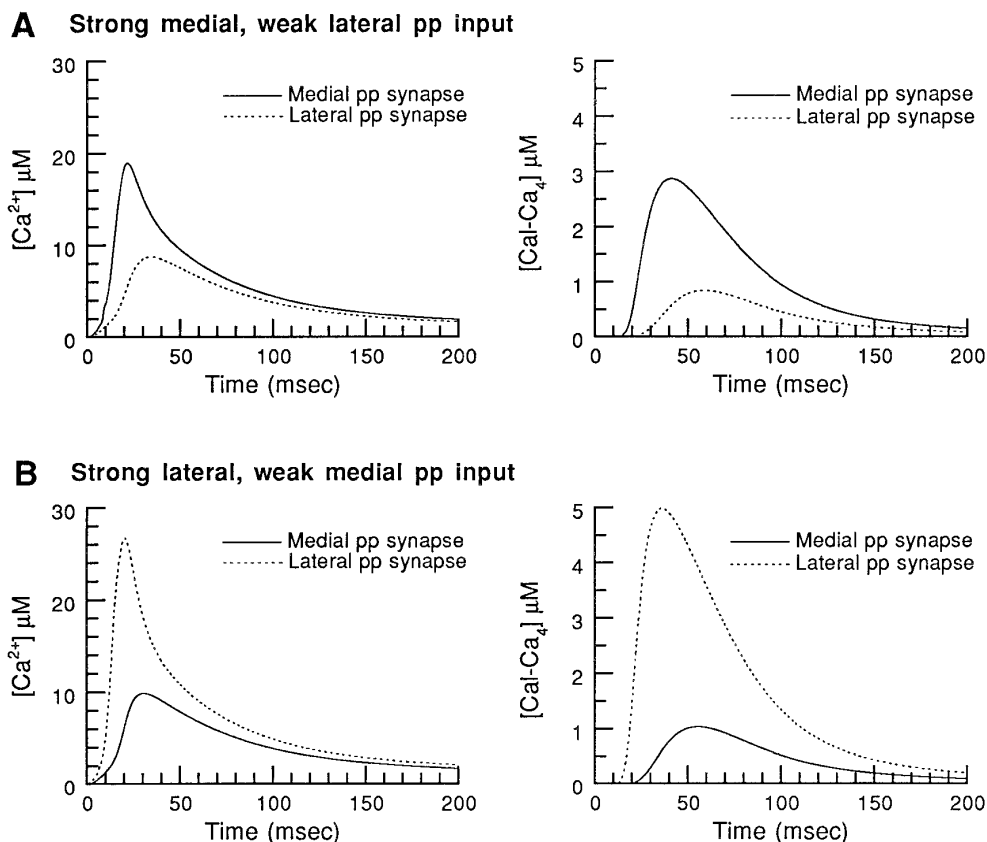


FIG. 3. Ca^{2+} concentration ($[\text{Ca}^{2+}]$) and $[\text{Cal-Ca}_4]$ in spine heads of weak and strong input path synapses when R_m at the soma and the distal 2/3 of the dendritic tree was reduced to $1,600 \Omega \text{ cm}^2$. Note that spine membrane R_m was not reduced. A: strong medial pp input (300 activated synapses) and weak lateral pp input (1 synapse). B: strong lateral pp input (264 activated synapses) and weak medial pp input (1 synapse).

obtained for stronger inhibition, suggesting that the result is somewhat robust physiologically in that more excitation would be accompanied by more inhibition.

Location of inhibition necessary for the spatial convergence requirement

In the above simulations R_m was reduced only in the soma and in the distal two-thirds of the dendritic tree. To determine whether other locations of shunting inhibition might be more consistent with the spatial convergence requirement, the value of R_m was changed 1) only in the distal two-thirds of the dendritic tree, 2) in the whole dendritic tree and the soma, 3) only in the middle third of the dendritic tree (region of medial pp input), or 4) only in the distal third of the dendritic tree (region of lateral pp input).

When R_m was changed only in the distal two-thirds of the dendritic tree and not at the soma, the ratio of peak $[\text{Cal-Ca}_4]$ values was larger when the medial pp was the strong input path and smaller when the lateral pp was the strong input path compared with the case when inhibition was also included at the soma. For example, the ratios of 3.5 and 4.8 shown in Fig. 3 became 3.9 (Fig. 6A) and 4.5 (Fig. 6B) when the reduced R_m was $1,600 \Omega \text{ cm}^2$. As one might expect, the value of R_m at the soma had more of an effect on $[\text{Cal-Ca}_4]$ in the medial pp synapse than in the more remote

lateral pp synapse. Nevertheless, qualitatively it made little difference for the spatial convergence requirement whether or not R_m was reduced at the soma as well as in the distal two-thirds of the dendritic tree.

When R_m was reduced in the soma and all dendrites, the ratio of peak $[\text{Cal-Ca}_4]$ values increased to 5.9 for strong lateral pp input and decreased to 2.6 for strong medial pp input compared with the case with inhibition only in the distal two-thirds of the dendritic tree and the soma. As expected, the reduced R_m in the proximal third of the dendritic tree had more of an effect on the medial pp input than on the lateral pp input. It would seem that this distribution of shunting inhibition would not be consistent with the spatial convergence requirement, although it would be an effective distribution to limit potentiation to lateral pp synapses following strong lateral pp input.

When reduced R_m or shunting inhibition was restricted to the middle third or to the distal third of the dendritic tree, results were not consistent with the spatial convergence requirement. With reduced R_m in the distal third of the dendritic tree, the ratio of peak $[\text{Cal-Ca}_4]$ values was large for strong medial pp input but small for strong lateral pp input. With reduced R_m in the middle third of the dendritic tree, the ratio of peak $[\text{Cal-Ca}_4]$ values was large with strong lateral pp input (but only for small R_m values) and close to 1.0 with strong medial pp input (Fig. 6).

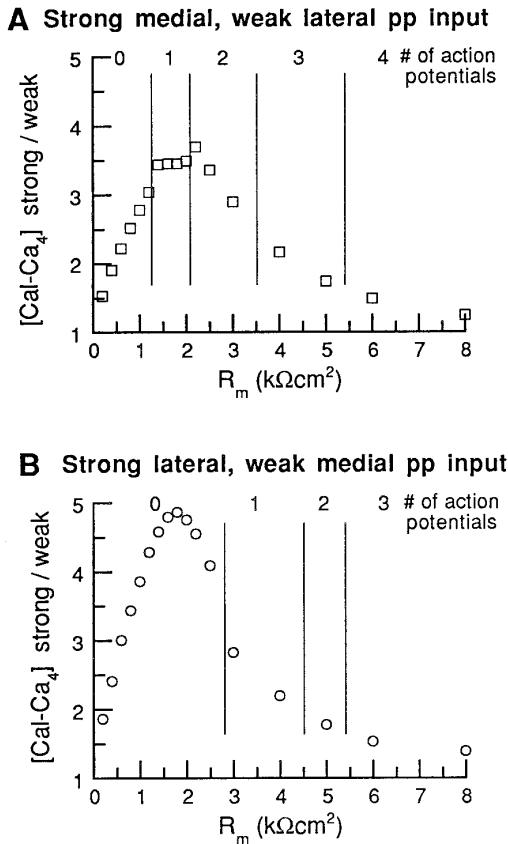


FIG. 4. Ratio of peak [Cal-Ca₄] in spine head of strong input path synapse to peak [Cal-Ca₄] in spine head of weak input path synapse as a function of reduced R_m at the soma and the distal 2/3 of the dendritic tree. Vertical lines isolate regions where same number of action potentials was generated. Numbers 0–4: number of action potentials generated. A: strong medial (300 synapses) and weak lateral (1 synapse) pp input. B: strong lateral (264 synapses) and weak medial (1 synapse) pp input. Synapses were activated 8 times at 400 Hz.

Taken together, these results suggest that pp input would have to activate inhibition in both the middle and distal thirds of the dendritic tree, regardless of whether it is medial or lateral pp input, if shunting inhibition is responsible for the spatial convergence requirement in these cells. The possibility that medial pp input activates inhibition only in the distal third and that lateral pp input activates inhibition only in the middle third of the dendritic tree is also consistent with the spatial convergence requirement, but such an anatomic arrangement seems unlikely.

Strength of inhibition in the middle and distal thirds of the dendritic tree

Although the above results suggest that shunting inhibition with pp activation exists in the distal two-thirds of the dendritic tree, it is not clear whether the strength of inhibition is the same in the middle and distal thirds. To address this issue we make the assumption that the spatial convergence requirement should be quantitatively symmetrical, i.e., the ratio of peak [Cal-Ca₄] values should be similar regardless of the source of the strong input. In results reported up to this point, the ratios typically have been larger for strong

lateral pp input than for strong medial pp input. To determine whether the strength of inhibition needed to get a quantitatively symmetrical spatial convergence requirement should be stronger, the same, or weaker in the middle third of the dendritic tree than in the distal third of the dendritic tree, simulations were performed with different R_m values in the two regions.

The simulation results predict that inhibition should be stronger in the distal third of the dendritic tree than in the middle third if the spatial convergence requirement is symmetrical. When R_m was lower in the middle third of the dendritic tree than in the distal third, there were larger differences in the ratios of peak [Cal-Ca₄] values with strong medial and strong lateral pp input than when R_m was the same in the two regions (Fig. 7). When R_m was lower in the distal third than in the middle third of the dendritic tree, the differences in the ratios became smaller. Because ratios become larger with a larger number of activated synapses, another way to make differences between the ratios for strong medial and strong lateral pp input smaller would be to increase the number of activated medial pp synapses and/or decrease the number of activated lateral pp synapses in the comparison. However, we already consider more activated

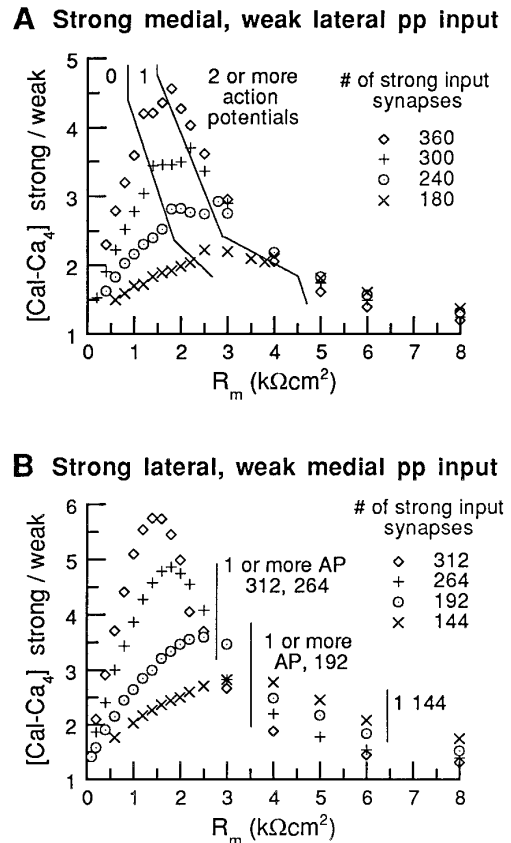


FIG. 5. Ratio of peak [Cal-Ca₄] at strong input path synapse to peak [Cal-Ca₄] at weak input path synapse as a function of reduced R_m for different numbers of activated synapses. A: strong medial and weak lateral pp input. Lines separate regions where 0, 1, or ≥ 2 action potentials were generated. B: strong lateral and weak medial pp input. Here lines merely indicate transition point between 0 and ≥ 1 action potentials (AP) for different numbers of activated synapses.

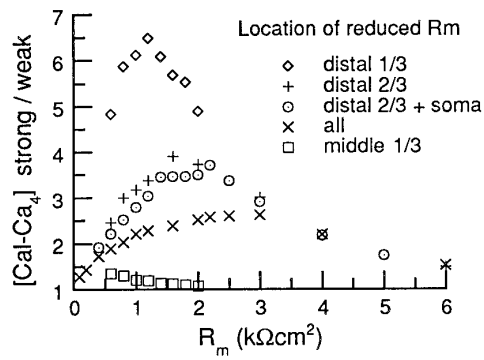
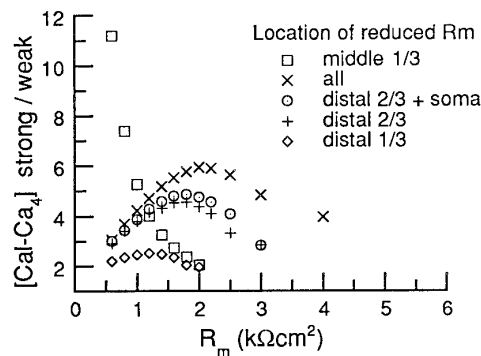
A Strong medial, weak lateral pp input**B Strong lateral, weak medial pp input**

FIG. 6. Ratio of peak $[Ca^{2+}]_i$ at strong input path synapse to peak $[Ca^{2+}]_i$ at weak input path synapse as a function of reduced R_m for different locations of reduced R_m . R_m was reduced either 1) only in the distal third of the dendritic tree, 2) only in the distal 2/3 of the dendritic tree, 3) in the distal 2/3 and soma, 4) everywhere, or 5) only in the middle third of the dendritic tree. Spine R_m was kept at $40,000 \Omega \text{ cm}^2$ in all simulations. A: strong medial (300 synapses) and weak lateral (1 synapse) pp input. B: strong lateral (264 synapses) and weak medial (1 synapse) pp input.

medial pp synapses than lateral pp synapses in our simulations.

Quantifying the number of inhibitory synapses activated by strong pp input

The values of R_m that maximized the spatial convergence requirement were used to estimate the amount of inhibition activated by pp input. Simulations were performed to check that the estimated number of inhibitory synapses and their frequency of activation would, indeed, satisfy the spatial convergence requirement.

The number of inhibitory synapses activated by pp input was computed with Eq. 5, assuming the $GABA_A$ kinetics in Eq. 3. A potential problem with this is that the parameter values used in Eq. 3 were taken from data on somatic synapses (DeKoninck and Mody 1994), and properties of dendritic $GABA_A$ synapses may be different (Soltesz et al. 1995). Consequently, we present ranges of values for the number of dendritic $GABA_A$ synapses assuming that their peak conductance may be as little as one-half that of somatic $GABA_A$ synapses. These ranges of values as a function of frequency of activation and target R_m value are given in

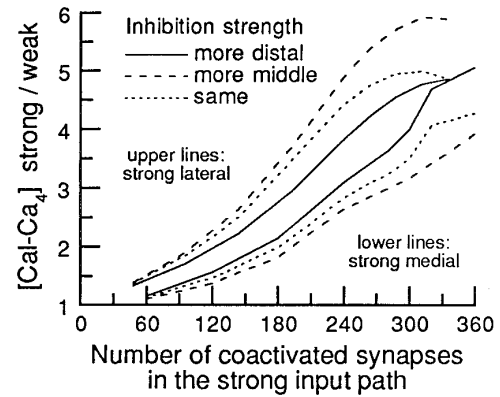


FIG. 7. Symmetrical spatial convergence requires more inhibition in the distal third than in middle third of the dendritic tree. Ratio of peak $[Ca^{2+}]_i$ at strong input path synapse to peak $[Ca^{2+}]_i$ at weak input path synapse is shown as a function of number of synapses activated in strong input path. For “more distal” inhibition, R_m was $2,200 \Omega \text{ cm}^2$ in the middle third of the dendritic tree and soma, and $1,600 \Omega \text{ cm}^2$ in the distal third. For “more middle” inhibition, R_m was $1,600 \Omega \text{ cm}^2$ in the middle third of the dendritic tree and soma, and $2,000 \Omega \text{ cm}^2$ in the distal third. For “same” inhibition, R_m was $2,000 \Omega \text{ cm}^2$ in the soma and distal 2/3 of the dendritic tree. Top 3 lines: results with strong lateral (264 synapses) and weak medial (1 synapse) pp input. Bottom 3 lines: results with strong medial (300 synapses) and weak lateral (1 synapse) pp input. With a symmetrical spatial convergence requirement, lines for strong lateral and strong medial pp input should coincide.

Table 2. With target R_m values of $2,200 \Omega \text{ cm}^2$ for the soma and middle third of the dendritic tree and $1,600 \Omega \text{ cm}^2$ for the distal third (as suggested from Figs. 5 and 7), eight-pulse, 400 Hz stimulation of 264 lateral pp or 300 medial pp excitatory synapses should also activate inhibition comparable with 76–145 inhibitory synapses activated at 100 Hz. The spatial distribution of these synapses should be 41–82 in the distal third of the dendritic tree, 28–56 in the middle third, and 7 at the soma.

When these inhibitory synapses were distributed over the cell in the model, there was considerable variation in the degree of match to the target R_m on individual dendrites. The addition of a single synapse could reduce the average R_m from $2,200$ to $1,600 \Omega \text{ cm}^2$, for example. Nevertheless, we distributed the synapses as best as we could to match the

TABLE 2. Number of inhibitory synapses activated

Target R_m , $\Omega \text{ cm}^2$	Frequency Interval, ms	Soma	Middle Third	Distal Third
1,600	4	6	24–48	26–52
	8	8	31–62	35–70
	10	9	38–76	41–82
1,800	4	5	22–44	23–46
	8	7	28–56	30–60
	10	8	34–68	37–74
2,000	4	5	19–38	21–42
	8	6	25–50	27–54
	10	8	31–62	33–66
2,200	4	4	18–36	19–38
	8	6	23–46	25–50
	10	7	28–56	30–60
2,400	4	4	16–32	18–36
	8	5	21–42	23–46
	10	6	25–50	28–56

R_m , membrane resistivity.

target R_m for each dendritic segment. Because the inhibitory synapses may not all be activated at the same times, we divided the synapses randomly into four groups. Activation in each group was at 100 Hz, with the time of the first activation being either 2, 5, 7, or 10 ms after the start of the pp input. The group with activation beginning at 10 ms was activated additionally at 5 ms.

The fact that target R_m was not matched exactly on every dendrite made it difficult to determine an optimal number of inhibitory synapses and synapse distribution to maximize the spatial convergence requirement for the particular pair of excitatory synapses being studied. With 76 inhibitory synapses activated at 100 Hz in the model at times noted above, peak $[\text{Cal-Ca}_4]$ at the strongly activated path synapse was 3.4 times higher for strong medial pp input and 4.1 times higher for strong lateral pp input than at the weakly activated path synapse. In an attempt to equalize the ratios, an additional inhibitory synapse was added distal to the lateral pp synapse (Fig. 8A). This made the ratio of peak $[\text{Cal-Ca}_4]$ values with strong medial pp input larger than that for strong lateral pp input (4.2 vs. 3.3). This additional synapse was moved along the dendrite proximally. When the additional inhibitory synapse was placed equally between the two observed locations, both ratios were increased, but the lack of symmetry was not improved (3.6 vs. 4.3). Only when the additional synapse was placed just proximal to the lateral pp synapse were the ratios close to equal (4.0 vs. 3.7) (Fig. 8B). Because of the large effects adding individual inhibitory synapses had on peak $[\text{Cal-Ca}_4]$ and the $[\text{Cal-Ca}_4]$ ratios, further tuning of the placement, activation frequency, and times of activation of inhibitory synapses to provide a more symmetrical spatial convergence requirement was not done.

Quantifying inhibition duration and timing

With the additional inhibitory synapse located as in Fig. 8B, the number of times each inhibitory input was activated at 100 Hz was varied to determine the minimum number needed to preserve the spatial convergence requirement.

It was found that the eight-pulse, 400 Hz tetanus to the pp should cause inhibitory synapses to be activated at least four times each. Peak $[\text{Cal-Ca}_4]$ values and the ratios of peak values between strong and weak input pathways were identical whether inhibitory synapses were activated 5 or 20 times at 100 Hz. When the number of times inhibitory synapses were activated was reduced to four, the peak $[\text{Cal-Ca}_4]$ values and the ratios were affected only marginally. However, substantial differences were found when inhibitory synapses were activated fewer than four times. In these cases the shunting effect of the inhibition was not complete (Fig. 9). When each inhibitory synapse was activated only twice and there was strong lateral pp input, the excitatory conductance was able to depolarize the cell again within 10 ms of the last inhibitory input, and the cell fired two action potentials (Fig. 9A). Activating inhibitory synapses three times shunted much of the residual excitation (Fig. 9, A and B), but not enough to prevent the ratios of peak $[\text{Cal-Ca}_4]$ values between strong and weak input path synapses from being reduced to 3.5 and 3.0 from the 4.0 and 3.7 values found above.

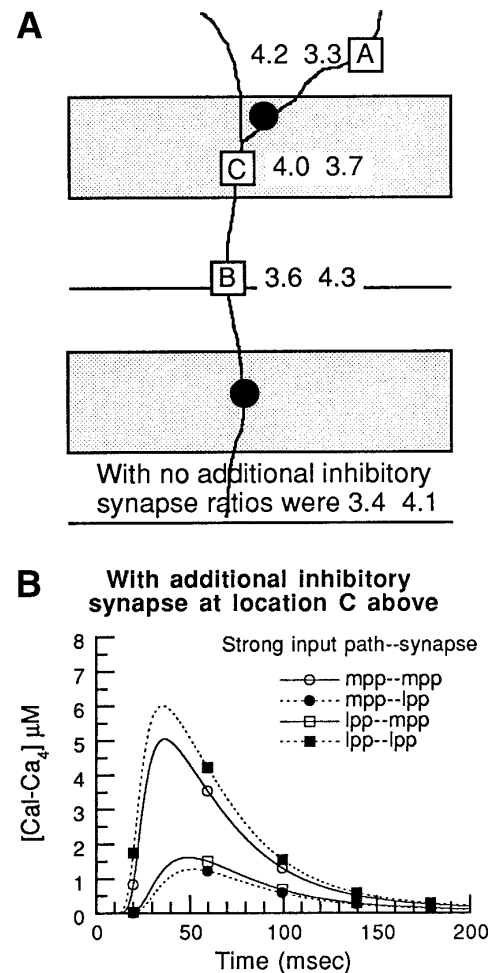


FIG. 8. Effect of adding single inhibitory synapses in model on $[\text{Cal-Ca}_4]$ in spine head. Forty-one γ -aminobutyric acid-A (GABA_A) synapses were uniformly distributed in the distal third of the dendritic tree, 28 in the middle third, and 7 at the soma. Synapses were activated at 100 Hz, with equal numbers starting at 2, 5, 7, and 10 ms after start of excitatory input. Group activated at 100 Hz starting at 10 ms was activated additionally at 5 ms. With this inhibition, the spatial convergence requirement was not symmetrical. *A*: 1 additional inhibitory synapse was added either at location A, B, or C. Additional inhibitory synapse placed at location C produced the most symmetrical spatial convergence requirement, as shown by ratios of peak $[\text{Cal-Ca}_4]$ values given at each location for strong medial pp and strong lateral pp input. *B*: $[\text{Cal-Ca}_4]$ is shown at medial and lateral pp synapses (mpp and lpp, respectively) for strong medial, weak lateral or strong lateral, weak medial pp activation. The 1st designation is strong input path and the 2nd is synapse. For example, mpp-lpp means strongly activated medial pp with $[\text{Cal-Ca}_4]$ plotted for lateral pp synapse.

The delay to the start of activation of inhibition was varied to determine how soon the inhibition had to be activated after the start of excitatory input to maintain the spatial convergence requirement.

It was found that most inhibitory synapses should be activated in the first 2–5 ms after the start of the pp input. In the baseline case, the first activation times of the four groups of inhibitory synapses were at 2, 5, 7, and 5 ms. When the first activation time of the last group was changed to 0 ms, the peak $[\text{Cal-Ca}_4]$ values and the ratio of peak values between strong and weak input pathways were changed only slightly (Fig. 10). When the first activation time of the last group was changed to 10 ms, the ratio of the peak $[\text{Cal-}$

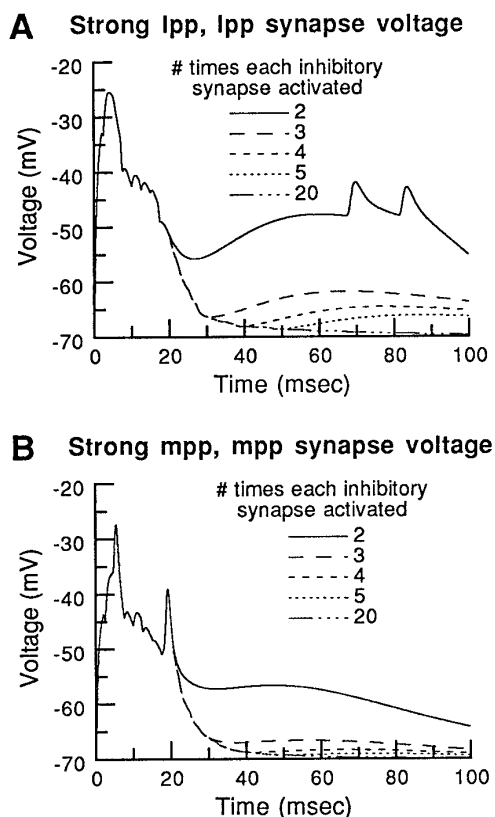


FIG. 9. Inhibitory synapses should be activated ≥ 4 times at 100 Hz for shunting inhibition to be effective. Inhibitory synapses were activated either 2, 3, 4, 5, or 20 times at 100 Hz. *A*: voltage at lateral pp synapse with strong lateral, weak medial pp activation. The 2 late peaks when inhibitory synapses were activated only 2 times are due to action potential invasion of the distal dendrite. *B*: voltage at medial pp synapse with strong medial, weak lateral pp activation. The 2 peaks near 5 and 20 ms are due to action potential invasion of the dendrite.

Ca_4] values dropped to 3.6 and 3.5. If, in addition, the first activation time of the first group were changed to 12 ms, the ratio of peak values dropped further to 3.2 and 2.7, with the much lower ratio for strong lateral pp input caused by generation of an action potential, which increased peak $[Ca-Ca_4]$ at the medial pp synapse. Further delays increased peak $[Ca-Ca_4]$ values and reduced the differences found at strongly and weakly activated path synapses until the differences resembled those in Fig. 2 when there was no inhibition.

DISCUSSION

Our initial goal was to determine the basis of the spatial convergence requirement for associative LTP, i.e., why co-activation of a strong ipsilateral pp input with a weak contralateral pp input will not induce associative LTP in the weak input path unless both inputs project to the same dendritic domain. Our previous dentate granule cell model (Holmes and Levy 1990a) did not include inhibition and was not consistent with this requirement. Our early attempts to explain the spatial convergence requirement with shunting inhibition (Holmes and Levy 1990b) failed because we did not include sufficient inhibition in the model. We underestimated what the descriptive terms substantial inhibition or powerful inhibition meant quantitatively. Once it was determined that

activation of a very powerful shunting inhibition could account for the spatial convergence requirement, we sought to quantify this inhibition. The experimental results of White et al. (1988, 1990) demonstrated a symmetry in this requirement. Neither strong lateral pp input paired with weak medial pp input nor strong medial pp input paired with weak lateral pp input would allow associative LTP of the weak input path. By making use of this symmetrical relationship, we were able to quantify the inhibition activated with eight-pulse, 400 Hz pp input. An important experimental constraint satisfied by the model was that cell firing is necessary to induce LTP of medial pp synapses with strong medial pp input, but cell firing is not necessary to induce LTP of lateral pp synapses with strong lateral pp input.

Numbers of inhibitory synapses activated by pp input

Anatomic data impose an upper limit on the number of inhibitory synapses on a dentate granule cell. Halasy and Somogyi (1993a) report that the number of GABA positive synapses constitutes $\sim 7.5\%$ of the total number of synapses in the molecular layer. Fiková et al. (1994) report percentages of 3.7, 6.1, and 9.8% for the inner, middle, and distal thirds of the molecular layer in a population of ethanol-sensitive mice. Assuming there are 4,000 synapses on a dentate granule cell, then these data suggest that ~ 300 are inhibitory. This means that the middle and distal thirds of the

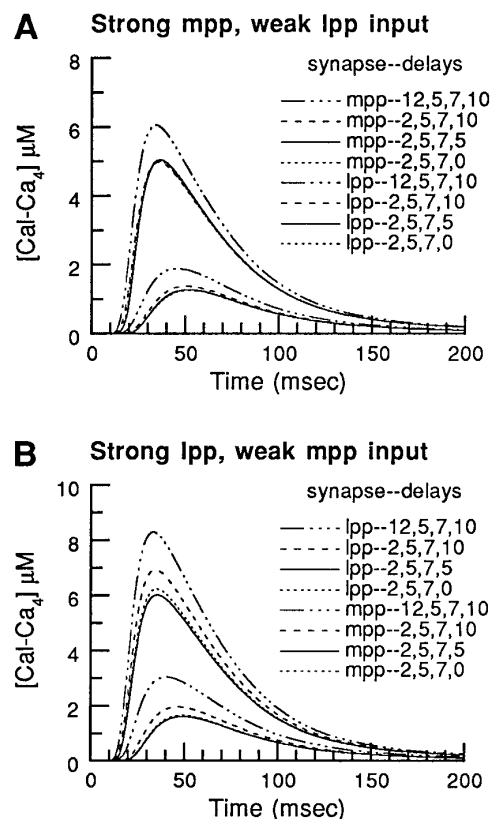


FIG. 10. Inhibition should be activated within 2–5 ms of activation of excitatory synapses. *A*: $[Ca-Ca_4]$ at medial and lateral pp synapses with strong medial, weak lateral pp input when 4 groups of inhibitory synapses were 1st activated at times indicated. *B*: $[Ca-Ca_4]$ with strong lateral, weak medial pp input.

dendritic tree will have ~80–120 inhibitory synapses each. Consequently, our results suggest that strong pp stimulation (8 pulses at 400 Hz) will activate 20–50% of the inhibitory synapses in the distal two-thirds of the dendritic tree depending on the frequency of inhibitory synapse activation.

Although this implies that a very large percentage of the inhibitory synapses in the cell is activated, this is not unreasonable because inhibition in the dentate has been reported previously to be quite powerful. Staley and Mody (1992) report a 5:1 ratio of GABAergic conductance to glutamatergic conductance in dentate granule cells following pp stimulation. It is difficult to compare this ratio directly with the model because of the different stimulation conditions, but given the 5- to 10-fold larger peak GABA_A conductance than peak α -amino-3-hydroxy-5-methyl-4-isoxazolepropionic acid (AMPA) conductance in the model, together with the longer GABA_A conductance duration and the smaller number of GABAergic synapses activated, then the inhibition is of similar magnitude. The results given here also show that more inhibition is activated as the strength of the pp activation is increased, as one might expect.

Furthermore, the amount of inhibition predicted by the model is consistent with LTP induction threshold parameters. LTP can be induced in the lateral pp with stimuli that are below the threshold for generation of a population spike as observed extracellularly. LTP in the medial pp requires a stimulus just above that which generates a population spike. The strength of inhibition suggested by the model prevents a strong lateral pp input from causing an action potential in the cell, but allows a strong medial pp input to generate one to two action potentials. Action potential generation provided a significant boost to calcium influx at medial pp synapses in the model even though dendrites in the distal two-thirds of the dendritic tree were passive. If lateral pp input were of sufficient strength to cause an action potential, the spatial convergence requirement would not be satisfied because of increased calcium influx at the medial pp synapse. The boost in depolarization at lateral pp synapses following an action potential is much smaller and has much less of an effect on calcium influx there.

Source of the inhibition

The model suggests that the source of the inhibition should be interneurons rather than direct connections of pp axons. Anatomic studies show that there is direct inhibitory input to the dentate via the pp (Germroth et al. 1989), but the number of connections is small and they are made mostly to the outer third of the dendritic tree. Results of the model are consistent with these data. The model results argue strongly against direct inhibitory connections in the medial pp because strong activation of the medial pp would then activate more inhibition in the middle third of the dendritic tree than in the distal third, and this would be inconsistent with the spatial convergence requirement. Conversely, direct inhibition in the lateral pp would not contradict the spatial convergence requirement as long as the inhibition is weak compared with that from interneurons.

For interneurons to be the source of this strong inhibition, interneurons must receive contacts from pp axons and have their axons terminating on granule cells in the distal two-

thirds of the dendritic tree. Anatomic studies suggest that the interneurons needed to provide this inhibition are present in the dentate. Interneurons having their dendrites and axons in the outer two-thirds of the molecular layer have been described (Buckmaster and Schwartzkroin 1995; Halasy and Somogyi 1993b; Han et al. 1993; Soriano and Frotscher 1993), and there is evidence that pp fibers form contacts on interneurons (Zipp et al. 1989). The axonal arborizations of some of these interneurons have been found to extend up to half of the total septotemporal length of the hippocampus (Buckmaster and Schwartzkroin 1995; Struble et al. 1978), suggesting that pp input might cause these cells to inhibit large parts of the dentate. In the model, inhibition at the soma was not essential for the spatial convergence requirement, although such inhibition may occur with pp input. The role of somatic inhibition was to delay or suppress action potential generation and shift slightly the amount of inhibition required to satisfy the spatial convergence requirement.

The firing patterns of inhibitory interneurons during an LTP-inducing stimulus are not known, but the model requires that interneurons fire in response to pp input even when the granule cells do not. Dentate hilar cells with dendrites in the molecular layer have been shown to have a lower threshold for activation by pp input than granule cells (Scharfman 1991), and it seems likely that this would be true for most interneurons because of their smaller size and larger input resistance. The model also requires that interneurons be able to fire at high frequencies in response to pp input. Scharfman and Schwartzkroin (1990) report that interneurons are able to fire at up to 1,000 Hz when stimulated at such a frequency, and the majority of interneurons does not show firing attenuation (Scharfman et al. 1990).

For effective shunting to take place, the model suggests that an eight-pulse, 400 Hz tetanus should cause inhibitory synapses to be activated four or more times. This does not seem to be an unreasonable number given the high excitability of interneurons noted above. Effective shunting also requires that the inhibition be activated within the first 5 ms after the pp synapses are activated. If fast-activated voltage-dependent sodium or calcium channels are present on these dendrites, then the delay to first activation may have to be shorter than found here.

Alternatively, some of the required inhibition could come from tonic release of GABA by interneurons forming synapses in the distal two-thirds of the dendritic tree. pp activation would still have to increase the frequency of this tonic release according to the strength of the stimulus. This persistent shunting inhibition would eliminate the need for precise timing of the activation of inhibition relative to the excitation. For this mechanism to work, interneurons forming synapses in the inner third of the dendritic tree should not release GABA tonically because this would not be consistent with the spatial convergence requirement. Because different interneurons form synapses in the inner third of the dendritic tree than in the outer two-thirds, this remains a possibility. Taken together with the reports mentioned above, the source of inhibition required by the model is likely to be present in the dentate.

Target of the inhibition

Although medial pp input provides excitation only to the middle third of the dendritic tree and lateral pp input provides excitation only to the distal third of the dendritic tree, either input should strongly activate inhibition in both the middle and distal thirds of the dendritic tree. This is not surprising, because the source of the inhibition is interneurons, and there is evidence for interneurons having their dendrites and axons in the outer two-thirds of the molecular layer as mentioned above. However, pp input should activate few or no inhibitory synapses in the inner third of the dendritic tree (at least within the 1st 50 ms). Such inhibition would also act against the spatial convergence requirement.

Inhibition should be stronger in the distal third of the dendritic tree than in the middle third. From cable theory, one expects severe voltage attenuation in the distal-to-proximal direction, but minor attenuation in the reverse direction (Rall 1989). Stronger inhibition is needed in the distal third to reduce the voltage there following input to the middle third of the dendritic tree. Anatomic studies provide a basis for stronger distal inhibition. Fiková et al. (1994) find that the percentage of GABAergic synapses in the distal third of the dendritic tree is higher than in the middle third. Chan-Palay (1978) reports that the highest density of GABA receptors in the dentate molecular layer, as determined by [³H]muscimol autoradiography, is in the distal third. Inhibition in the distal third might even be stronger than suggested here if the release of opioid peptides with lateral pp activation reduces inhibition in the distal third (Bramham 1992). This mechanism would strengthen the spatial convergence requirement.

Sculpting role of inhibition

Inhibition can play a role in limiting potentiation to particular dendritic regions, particular dendrites within regions, and even to particular synapses. If inhibition is activated in all regions of the dendritic tree, then the distal third acts as an independent unit with regards to potentiation, but the middle third does not. If inhibition is activated in the outer two-thirds of the dendritic tree, both the middle third and distal thirds may act as independent units. This might be desirable if the medial and lateral entorhinal cortex convey different types of information. On particular dendrites, addition or deletion of inhibitory synapses may change [Cal-Ca₄] levels in all excitatory synapses on the dendrite and thus affect potentiation there. Within a dendrite, addition of a single inhibitory synapse may control peak [Cal-Ca₄] in a single synapse or a small group of synapses. Control may occur at a finer level if extrasynaptic GABA_A receptors are present and are activated. This potential physiological role for extrasynaptic GABA_A receptors could ameliorate the difficulty we had with distributing the necessary dendritic GABA_A synapses to maximize the spatial convergence requirement.

Criteria for LTP induction

In Holmes and Levy (1990a), the criteria for LTP induction was peak spine head [Ca²⁺], and a steep nonlinearity in spine head [Ca²⁺] occurred once the spine head calcium

buffer became saturated. With conditions thought to induce LTP, peak spine head [Ca²⁺] in the model reached 20–30 μM, consistent with values recently obtained experimentally (Petrozzino et al. 1995). However, the buffer rate constants were different here. Calmodulin was assumed to be the primary buffer, and the rate constants estimated by Linse et al. (1991) for the binding of calcium to calmodulin were used in this study. Although peak spine head [Ca²⁺] values in the model are still 20–30 μM, we now see only a 2-fold difference in spine head [Ca²⁺] when modeling stimulation conditions that do and do not lead to LTP (see Fig. 3), whereas a 10-fold difference was found with the old model. This suggests that buffer saturation may no longer be an attractive hypothesis to explain LTP induction, and also that it may not be so easy to distinguish between calcium levels thought to lead to LTP or long-term depression (Neveu and Zucker 1996). Nevertheless, two-fold differences may imply the existence of a (non-calmodulin-dependent) reaction catalyzed by high concentrations of calcium. However, in the present model we extended the measure for LTP induction to include peak [Cal-Ca₄] as well as peak [Ca²⁺], and found that two-fold differences in peak spine head [Ca²⁺] were magnified into four-fold differences in peak [Cal-Ca₄]. We assume that these differences will be magnified further by subsequent biochemical reactions.

Comments about the model

There are several other factors affecting peak spine head [Cal-Ca₄] values that may need to be included in future models. There is some evidence that the synaptic conductances at medial and lateral pp synapses are different (Abraham and McNaughton 1984; McNaughton 1980). Because we do not have the data to quantify these differences at present, we assumed that the conductance kinetics were identical at all excitatory synapses. Although synaptic conductances were computed from receptor binding equations instead of the usual double-exponential functions, it is not clear that the NMDA conductance is represented adequately. It may be necessary to include glycine in the binding reaction equations. Perhaps a more important problem is that the probability of transmitter release may be highly variable among synapses (Hessler et al. 1993), whereas here it is assumed to be 1.0 for all synapses. This problem may be minimized here because the results depend on the interaction of excitation and inhibition, and the effect of making release probability variable for both types of synapses may cancel out. This needs to be studied further. Finally, the results reported were obtained without voltage-dependent conductances in most of the dendritic tree, and voltage-dependent conductances have been found in dendrites of hippocampal cells (Magee and Johnston 1995; Spruston et al. 1995). However, the densities of such conductances in dentate granule cells are thought to be much lower than in CA1 or CA3 pyramidal cells (Fricke and Prince 1984). Work by Jefferys (1979) suggests that action potentials back-propagate to the middle third but not to the distal third of dentate granule cells. However, in the present simulations with passive dendrites, depolarization caused by action potentials is substantially larger in the middle third than in the distal third of the dendritic tree (Fig. 9). Preliminary calculations suggest that

the densities of dendritic voltage-dependent conductances required to reproduce the Jefferys result are very low and that including them would not change the conclusions of the present study, but further work is needed. Nevertheless, results of the present model suggest that pp input can activate interneurons to provide powerful inhibition to dentate granule cells. This inhibition can isolate potentiated synapses to particular dendritic domains, and the location of activated inhibitory synapses may affect potentiation of individual synapses on individual dendrites.

We acknowledge helpful discussions and preliminary investigations of a variety of models of inhibition with O. Yousukhno.

This work was supported by National Institutes of Health Grants MH-51081 to W. R. Holmes and NS-15488, MH-48161, and MH-00622; by Electric Power Research Institute RP8030-08; by Pittsburgh Supercomputing Center Grant BNS950001 to W. B. Levy; and by the Department of Neurosurgery, University of Virginia.

Address for reprint requests: W. R. Holmes, Neurobiology Program, Dept. of Biological Sciences, Ohio University, Athens, OH 45701.

Received 15 October 1996; accepted in final form 6 March 1997.

REFERENCES

- ABRAHAM, W. C. AND MCNAUGHTON, N. Differences in synaptic transmission between medial and lateral components of the perforant path. *Brain Res.* 303: 251–260, 1984.
- ASCHER, P. AND NOWAK, L. The role of divalent cations in the *N*-methyl-D-aspartate responses of mouse central neurones in culture. *J. Physiol. Lond.* 399: 247–266, 1988.
- BLAXTER, T. J. AND CARLEN, P. L. GABA responses in rat dentate granule neurons are mediated by chloride. *Can. J. Physiol. Pharmacol.* 66: 637–642, 1988.
- BLISS, T. V. P. AND LOMO, T. Long-lasting potentiation of synaptic transmission in the dentate area of the anaesthetized rabbit following stimulation of the perforant path. *J. Physiol. Lond.* 232: 331–356, 1973.
- BRAMHAM, C. R. Opioid receptor dependent long-term potentiation: peptidergic regulation of synaptic plasticity in the hippocampus. *Neurochem. Int.* 20: 441–445, 1992.
- BUCKMASTER, P. S. AND SCHWARTZKROIN, P. A. Interneurons and inhibition in the dentate gyrus of the rat in vivo. *J. Neurosci.* 15: 774–789, 1995.
- CHAN-PALAY, V. Quantitative visualization of gamma-aminobutyric acid receptors in hippocampus and area dentata demonstrated by [³H] muscimol autoradiography. *Proc. Natl. Acad. Sci. USA* 75: 2516–2520, 1978.
- DEKONINCK, Y. AND MODY, I. Noise analysis of miniature IPSCs in adult rat brain slices: properties and modulation of synaptic GABA_A receptor channels. *J. Neurophysiol.* 71: 1318–1335, 1994.
- FIFKOVÁ, E., EASON, H., BUELTMANN, K., AND LANMAN, J. Changes in GABAergic and non-GABAergic synapses during chronic ethanol exposure and withdrawal in the dentate fascia of LS and SS mice. *Alcoholism NY* 18: 989–997, 1994.
- FRICKE, R. A. AND PRINCE, D. A. Electrophysiology of dentate gyrus granule cells. *J. Neurophysiol.* 51: 195–209, 1984.
- GERMROTH, P., SCHWERDTFEGER, W. K., AND BUHL, E. H. GABAergic neurons in the entorhinal cortex project to the hippocampus. *Brain Res.* 494: 187–192, 1989.
- HALASY, K. AND SOMOGYI, P. Distribution of GABAergic synapses and their targets in the dentate gyrus of rat: a quantitative immunoelectron microscopic analysis. *J. Hirnforsch.* 34: 299–308, 1993a.
- HALASY, K. AND SOMOGYI, P. Subdivisions in the multiple GABAergic innervation of granule cells in the dentate gyrus of the rat hippocampus. *Eur. J. Neurosci.* 5: 411–429, 1993b.
- HAN, Z.-S., BUHL, E. H., LÖRINCZI, Z., AND SOMOGYI, P. A high degree of spatial selectivity in the axonal and dendritic domains of physiologically identified local-circuit neurons in the dentate gyrus of the rat hippocampus. *Eur. J. Neurosci.* 5: 395–410, 1993.
- HESSLER, N. A., SHIRKE, A. M., AND MALINOW, R. The probability of transmitter release at a mammalian central synapse. *Nature Lond.* 366: 569–572, 1993.
- HOLMES, W. R. Is the function of dendritic spines to concentrate calcium? *Brain Res.* 519: 338–342, 1990.
- HOLMES, W. R. Modeling the effect of glutamate diffusion and uptake on NMDA and non-NMDA receptor saturation. *Biophys. J.* 69: 1734–1747, 1995.
- HOLMES, W. R. AND LEVY, W. B. Insights into associative long-term potentiation from computational models of NMDA receptor-mediated calcium influx and intracellular calcium concentration changes. *J. Neurophysiol.* 63: 1148–1168, 1990a.
- HOLMES, W. R. AND LEVY, W. B. Insights into LTP from computational models. Synaptic input distributions and spine head [Ca²⁺]. *Soc. Neurosci. Abstr.* 16: 493, 1990b.
- HOLMES, W. R. AND LEVY, W. B. Temporal requirement for associative LTP in the dentate. Dependence on modeled R_m and R_i values. In: *Computation in Neurons and Neural Systems*, edited by F. Eeckman. Boston, MA: Kluwer, 1994, p. 299–304.
- JEFFERYS, J. G. Initiation and spread of action potentials in granule cells maintained in vitro in slices of guinea-pig hippocampus. *J. Physiol. Lond.* 289: 375–388, 1979.
- JONAS, P., MAJOR, G., AND SAKMANN, B. Quantal components of unitary EPSCs at the mossy fibre synapse on CA3 pyramidal cells of rat hippocampus. *J. Physiol. Lond.* 472: 615–663, 1993.
- LINSE, S., HELMERSSON, A., AND FORSEN, S. Calcium binding to calmodulin and its globular domains. *J. Biol. Chem.* 266: 8050–8054, 1991.
- MAGEE, J. C. AND JOHNSTON, D. Synaptic activation of voltage-gated channels in the dendrites of hippocampal pyramidal neurons. *Science Wash. DC* 268: 301–304, 1995.
- MALENKA, R. C. AND NICOLL, R. A. NMDA-receptor-dependent synaptic plasticity: multiple forms and mechanisms. *Trends Neurosci.* 16: 521–527, 1993.
- MAYER, M. L. AND WESTBROOK, G. L. Permeation and block of *N*-methyl-D-aspartic acid receptor channels by divalent cations in mouse cultured central neurones. *J. Physiol. Lond.* 394: 501–527, 1987.
- MCNAUGHTON, B. L. Evidence for two physiologically distinct perforant pathways to the fascia dentata. *Brain Res.* 199: 1–19, 1980.
- MCNAUGHTON, B. L., BARNES, C. A., AND ANDERSEN, P. Synaptic efficacy and EPSP summation in granule cells of rat fascia dentata studied in vitro. *J. Neurophysiol.* 46: 952–966, 1981.
- NEVEU, D. AND ZUCKER, R. S. Postsynaptic levels of [Ca²⁺]_i needed to trigger LTD and LTP. *Neuron* 16: 619–629, 1996.
- OTIS, T. S. AND MODY, I. Modulation of decay kinetics and frequency of GABA_A receptor-mediated spontaneous inhibitory postsynaptic currents in hippocampal neurons. *Neuroscience* 49: 13–32, 1992.
- PETROZZINO, J. J., POZZO-MILLER, L. D., AND CONNOR, J. A. Micromolar Ca²⁺ transients in dendritic spines of hippocampal pyramidal neurons in brain slice. *Neuron* 14: 1223–1231, 1995.
- RALL, W. Cable theory for dendritic neurons. In: *Methods in Neuronal Modeling*, edited by C. Koch and I. Segev. Cambridge, MA: MIT Press, 1989, p. 9–62.
- RALL, W., BURKE, R. E., HOLMES, W. R., JACK, J. J. B., REDMAN, S. J., AND SEGEV, I. Matching dendritic neuron models to experimental data. *Physiol. Rev.* 72, Suppl. 4: 159–186, 1992.
- SATHER, W., DIEUDONNE, S., MACDONALD, J. F., AND ASCHER, P. Activation and desensitization of *N*-methyl-D-aspartate receptors in nucleated outside-out patches from mouse neurones. *J. Physiol. Lond.* 450: 643–672, 1992.
- SCHARFMAN, H. E. Dentate hilar cells with dendrites in the molecular layer have lower thresholds for synaptic activation by perforant path than granule cells. *J. Neurosci.* 11: 1660–1673, 1991.
- SCHARFMAN, H. E., KUNKEL, D. D., AND SCHWARTZKROIN, P. A. Synaptic connections of dentate granule cells and hilar neurons: results of paired intracellular recordings and intracellular horseradish peroxidase injections. *Neuroscience* 37: 693–707, 1990.
- SCHARFMAN, H. E. AND SCHWARTZKROIN, P. A. Responses of cells of the rat fascia dentata to prolonged stimulation of the perforant path: sensitivity of hilar cells and changes in granule cell excitability. *Neuroscience* 35: 491–504, 1990.
- SOLTESZ, I., SMETTERS, D. K., AND MODY, I. Tonic inhibition originates from synapses close to the soma. *Neuron* 14: 1273–1283, 1995.
- SORIANO, E. AND FROTSCHER, M. GABAergic innervation of the rat fascia dentata: a novel type of interneuron in the granule cell layer with extensive axonal arborization in the molecular layer. *J. Comp. Neurol.* 334: 385–396, 1993.
- SPRUSTON, N. AND JOHNSTON, D. Perforated patch-clamp analysis of the passive membrane properties of three classes of hippocampal neurons. *J. Neurophysiol.* 67: 508–529, 1992.

- SPRUSTON, N., SCHILLER, Y., STUART, G., AND SAKMANN, B. Activity-dependent action potential invasion and calcium influx into hippocampal CA1 dendrites. *Science Wash. DC* 268: 297–300, 1995.
- STALEY, K. J. AND MODY, I. Shunting of excitatory input to dentate gyrus granule cells by a depolarizing GABA_A receptor-mediated postsynaptic conductance. *J. Neurophysiol.* 68: 197–212, 1992.
- STALEY, K. J., OTIS, T. S., AND MODY, I. Membrane properties of dentate gyrus granule cells: comparison of sharp microelectrode and whole-cell recordings. *J. Neurophysiol.* 67: 1346–1358, 1992.
- STRUBLE, R. G., DESMOND, N. L., AND LEVY, W. B. Anatomical evidence for interlamellar inhibition in the fascia dentata. *Brain Res.* 152: 580–585, 1978.
- TOMASULO, R. A., RAMIREZ, J. J., AND STEWARD, O. Synaptic inhibition regulates associative interactions between afferents during the induction of long-term potentiation and depression. *Proc. Natl. Acad. Sci. USA* 90: 11578–11582, 1993.
- WHITE, G., LEVY, W. B., AND STEWARD, O. Evidence that associative interactions between synapses during the induction of long-term potentiation occur within local dendritic domains. *Proc. Natl. Acad. Sci. USA* 85: 2368–2372, 1988.
- WHITE, G., LEVY, W. B., AND STEWARD, O. Spatial overlap between populations of synapses determines the extent of their interaction during the induction of long-term potentiation and depression. *J. Neurophysiol.* 64: 1186–1198, 1990.
- YOUSUKHNO, O. V., HOLMES, W. R., AND LEVY, W. B. On the role of dendritic inhibition in associative LTP. In: *Computational Neuroscience*, edited by J. M. Bower. San Diego, CA: Academic, 1996, p. 95–100.
- YUEN, G.L.F. AND DURAND, D. Reconstruction of hippocampal granule cell electrophysiology by computer simulation. *Neuroscience* 41: 411–423, 1991.
- ZHANG, D. X. AND LEVY, W. B. Bicuculline permits the induction of long-term depression by heterosynaptic, translaminar conditioning in the hippocampal dentate gyrus. *Brain Res.* 613: 309–312, 1993.
- ZIPP, F., NITSCH, R., SORIANO, E., AND FROTSCHER, M. Entorhinal fibers form synaptic contacts on parvalbumin-immunoreactive neurons in the rat fascia dentata. *Brain Res.* 495: 161–166, 1989.